

Cooperative porphyrin-quadrupolar based triad for combined two-photon induced fluorescence and singlet oxygen generation

Jean-Baptiste Verlhac*, Guillaume Clermont and Mireille Blanchard-Desce*[†]

Université de Bordeaux, Institut des Sciences Moléculaires, UMR5255(CNRS), Bat A11, 351 Crs de la Libération, 33405 TALENCE CEDEX, France

Received 8 September 2016

Accepted 28 September 2016

ABSTRACT: The design and synthesis of a cooperative multichromophoric triad system which combines the large two-photon absorption properties of fluorene-cored bis-donor quadrupolar dyes and the remarkable sensitizing properties of the porphyrin subunit (*i.e.* high intersystem crossing and ability to produce singlet oxygen by energy transfer to oxygen from its triplet excited state) is described. After irradiation the energy can be transferred from the quadrupolar chromophores to the porphyrin with an estimated 80% efficiency *via* a FRET process. Moreover both the two-photon absorption properties of the quadrupolar subunits and the sensitizing and fluorescence properties of the porphyrin are retained indicating that deleterious competing processes (such as photo-induced electron transfer) are prevented in such molecular architectures thanks to the implemented design. As a result, the two-photon absorption induced singlet oxygen generation efficiency of the triad in the NIR region is found to be enhanced by an order of magnitude as compared to the porphyrin subunit. Potential applications of these porphyrin-based multichromophoric systems for photodynamic therapy based upon two-photon excitation in the NIR region might be possible since it overcomes the low two-photon absorption response of porphyrin while fully retaining their remarkable photosensitizing properties.

KEYWORDS: porphyrins, fluorene, quadrupolar, fluorescence, PDT, FRET.

INTRODUCTION

Photodynamic therapy (PDT) [1, 2] is a minimally invasive process used in oncology as an adjuvant treatment to surgery, chemotherapy or radiotherapy. This technique is also useful in ophthalmology for the treatment of the wet form of age-related macular degeneration (ARMD) [3]. The use of two-photon (2P) excitation allows the excitation of the photosensitizer to proceed only in the small volume around the focal spot of the focused laser beam, reducing damages away from the focus and thus permitting more localized treatment with 3D spatial

resolution. Moreover, the ability to create excited states with photons of half the energy allows excitation within the biological transparency region (700–1000 nm), increasing light penetration deeper into biological tissues [4, 5]. Optimized features for 2P photosensitizers are large cross sections in the biological spectral window as well as high singlet oxygen quantum yield in order to induce oxidative damages to the tumor cells. In addition, using sensitizers with much larger two-photon absorption cross sections than endogenous chromophores (whose TPA cross section maxima in the biological window are typically in the range 10^{-5} – 1 GM) [6] opens the way to more selective photo-addressing since two-photon absorption cross sections can be enhanced much more dramatically *via* molecular engineering than one-photon absorption cross sections [7]. In addition, if the sensitizers also exhibit fluorescence properties, they offer potential for combined imaging and therapy [5].

[†]SPP full member in good standing

*Correspondence to: Jean-Baptiste Verlhac, tel: +33 540-006-571, email: jean-baptiste.verlhac@u-bordeaux.fr; Mireille Blanchard-Desce, tel: +33 540-006-732, email: mireille.blanchard-desce@u-bordeaux.fr

Porphyrin derivatives, such as porfimer sodium (Photofrin®) and verteporfin (Visudyne®) are used in clinical trials because they exhibit high singlet oxygen quantum yields and reduced toxicity in the absence of light. However, these derivatives as well as the model tetraphenyl porphyrin (TPP) exhibit modest 2P absorption cross sections (10 to 50 GM) [8, 9]. These low 2PA cross section values thus require higher excitation power which can be deleterious and produces side damages. Various successful strategies have been proposed to enhance the 2PA cross sections using conjugated porphyrin dimers or oligomers [10], fused or bridged porphyrins [11] and porphyrin derivatives such as tetraazaporphyrins [12] and expanded porphyrins [13] and more generally porphyrin arrays [14] or *via* dissymmetrization [15, 16]. The effect of the extension of conjugation in expanded porphyrins is to broaden and red-shift the Q-bands from the visible to the NIR region resulting in the overlap of the 2PA band located in the NIR region with red-shifted one-photon absorption. This may distort two-photon absorption measurements and lead to overestimated apparent 2PA responses and to the loss of the high spatial resolution offered by 2P excitation as the nonlinear excitation process is competing with one-photon excitation. In addition, shifting the lowest excited state to lower energy also affects the excited states manifold. This is liable to affect the properties of the lowest excited state and reduce the intersystem crossing as well as the triplet state properties (*i.e.* its ability to generate singlet oxygen *via* a triplet–triplet energy transfer). In many occurrences, this causes a dramatic loss of fluorescence. An alternative strategy is based on the electronic disconnection between an octupolar- or quadrupolar-type core 2P absorber and peripheral porphyrins. These systems show total core-to-periphery through-bond energy transfer and retain the fluorescence and singlet oxygen generation of porphyrins [17].

An attractive approach in order to enhance the 2PA cross section of porphyrin derivatives without affecting their photophysical properties is to take advantages of FRET process. The FRET strategy relies on coupling 2PA antenna-chromophores with large 2PA response either to a fluorescent emitter (for 2P imaging) or a sensitizer (for 2P PDT) to which the antenna is able to transfer its excitation energy. In particular, there have been several reports on energy transfer (ET) in branched or dendritic systems in which the energy from 2P absorbers is transferred to the red-emitting core [18], or to a porphyrin core [19]. In particular, this strategy has been successfully applied to the design of *in vivo* sensitive oxygen 2P absorbing nanosensors by Vinogradov and co-workers by combining a Pt-porphyrin core with multiple coumarin chromophores (which act as 2P antenna) within a biocompatible dendritic architecture [20].

In our group, we have previously developed a strategy for the design of multichromophoric dendritic species *via* thiophosphoramidate bonds that allows duplication

of the number of chromophoric unit at each generation [21, 22]. In such dedicated dendrimeric architectures, ultrafast excitation energy transfer [23] or cooperative enhancement of 2P absorption [24] can be achieved *via* the use of specifically engineered 2P absorbing chromophoric subunits. Recently, we also reported the design of FRET-based dyads [25] and triads [26] which yielded enhanced 2P uncaging of acids, including neuroaminoacids. Extending this concept, we herein describe the design, synthesis and properties of a porphyrin based triad having a porphyrin linked to two quadrupolar 2PA chromophores *via* a thiophosphoramidate bond (Scheme 1).

RESULTS AND DISCUSSION

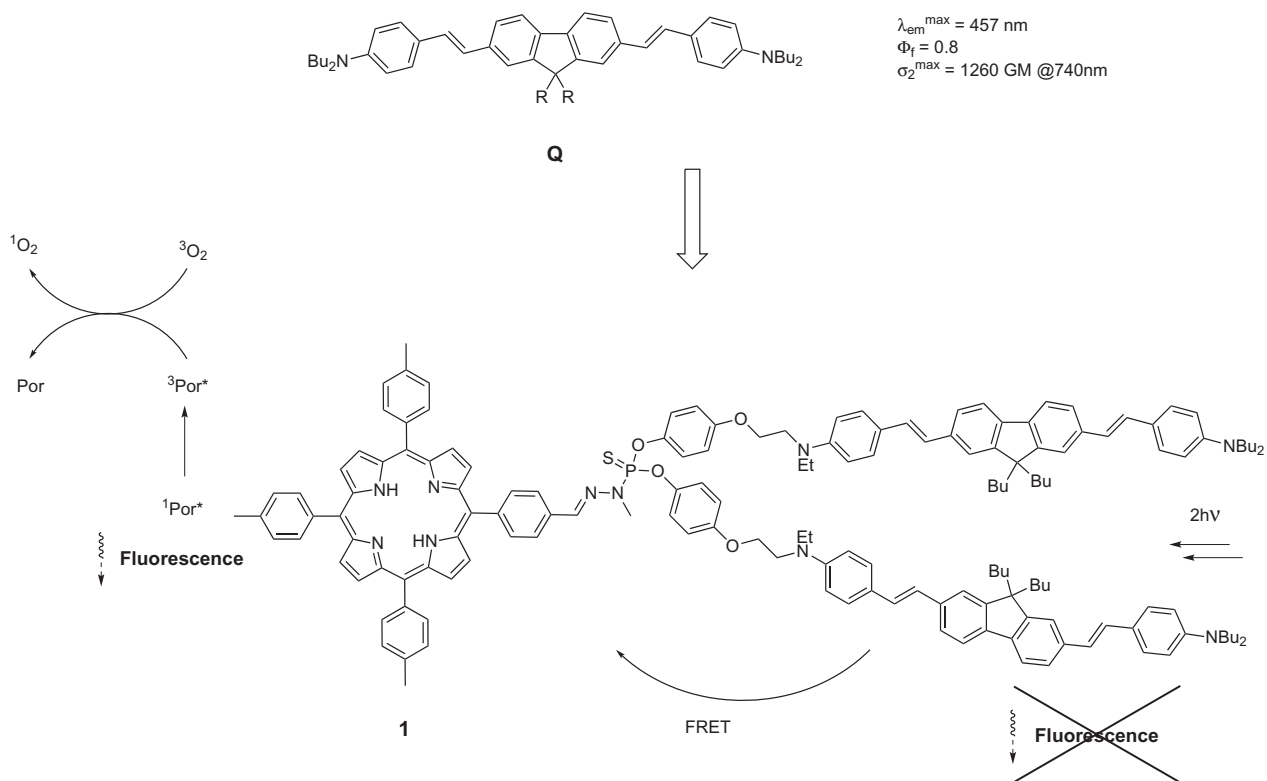
Design and synthesis

The schematic synthetic pathway is described in Scheme 2. Porphyrin precursor **5** is prepared *via* a four step procedure starting from commercially available derivatives. The preparation of the key intermediate aldehyde **4** has been already reported. It is obtained *via* a classical unsymmetrical Adler condensation of pyrrole with a 3/1 mixture of *para*-tolualdehyde and 4-carbomethoxybenzaldehyde in propionic acid [27]. The expected isomer **1** is obtained with a 6% yield by column chromatography of the crude reaction mixture. Reduction of the ester function by LiAlH₄ and subsequent oxidation of the benzylic alcohol function led to the aldehyde **4** according to published procedure for TPP-CHO [28]. Introduction of the dichlorothiophosphoramidate function is done by simple mixing of the hydrazine precursor with **4** in dichloromethane.

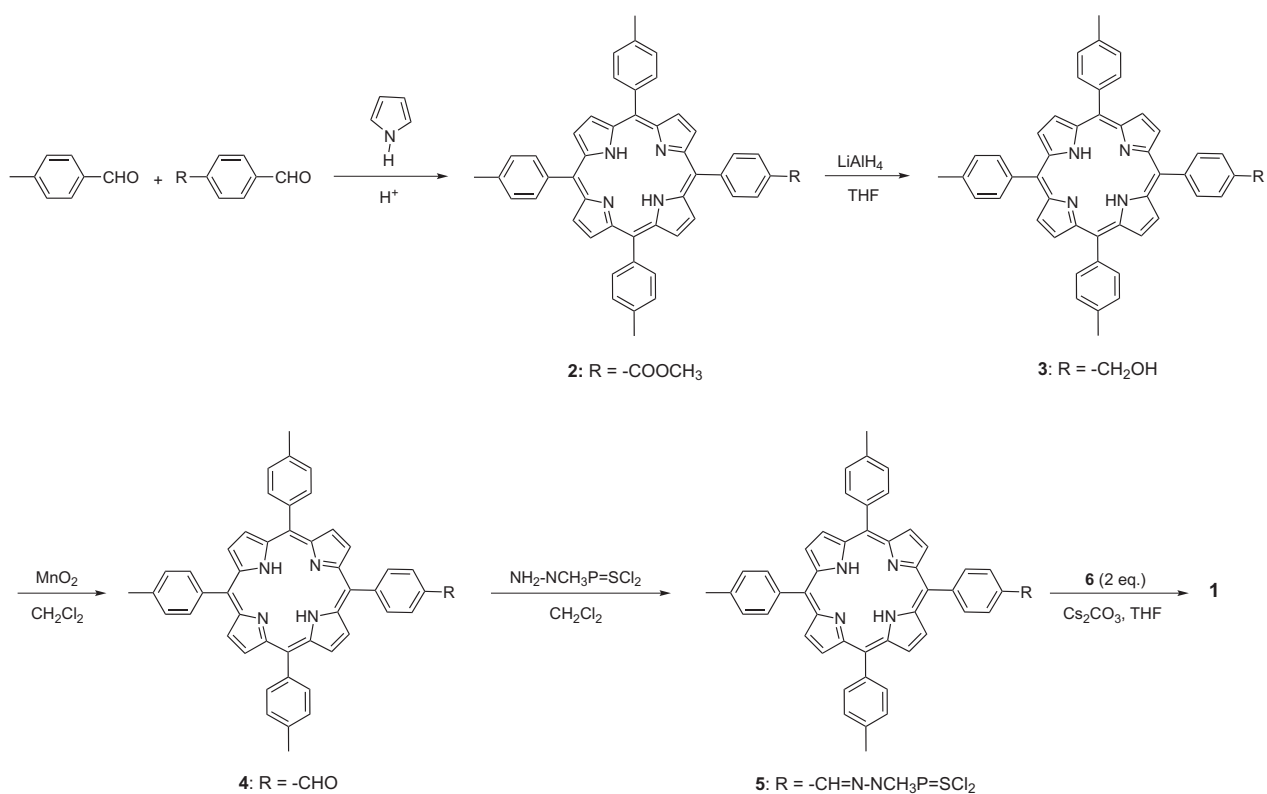
The dissymmetrical functionalized quadrupolar derivative **6** is prepared following the multistep synthesis described in Scheme 3. The methodology used to prepare this compound has been described previously for the preparation of an analog compound with C–C triple bond spacers instead of C–C double bonds [29]. Here we used a dissymmetrical Heck reaction instead of a Sonogashira coupling reaction and proceeded by a combinatorial approach which relies on the subsequent purification of the mixture of dissymmetrical target compound and symmetrical side products. Thanks to the presence of the phenol moiety, the three different products (**6**, **10** and **11**) could be easily separated by column chromatography.

Finally, reaction of two equivalents of the phenol moieties from functionalized quadrupolar derivative **6** with the two P–Cl bonds of porphyrin derivative **5** in the presence of Cs₂CO₃ led to triad **1** with 83% yield.

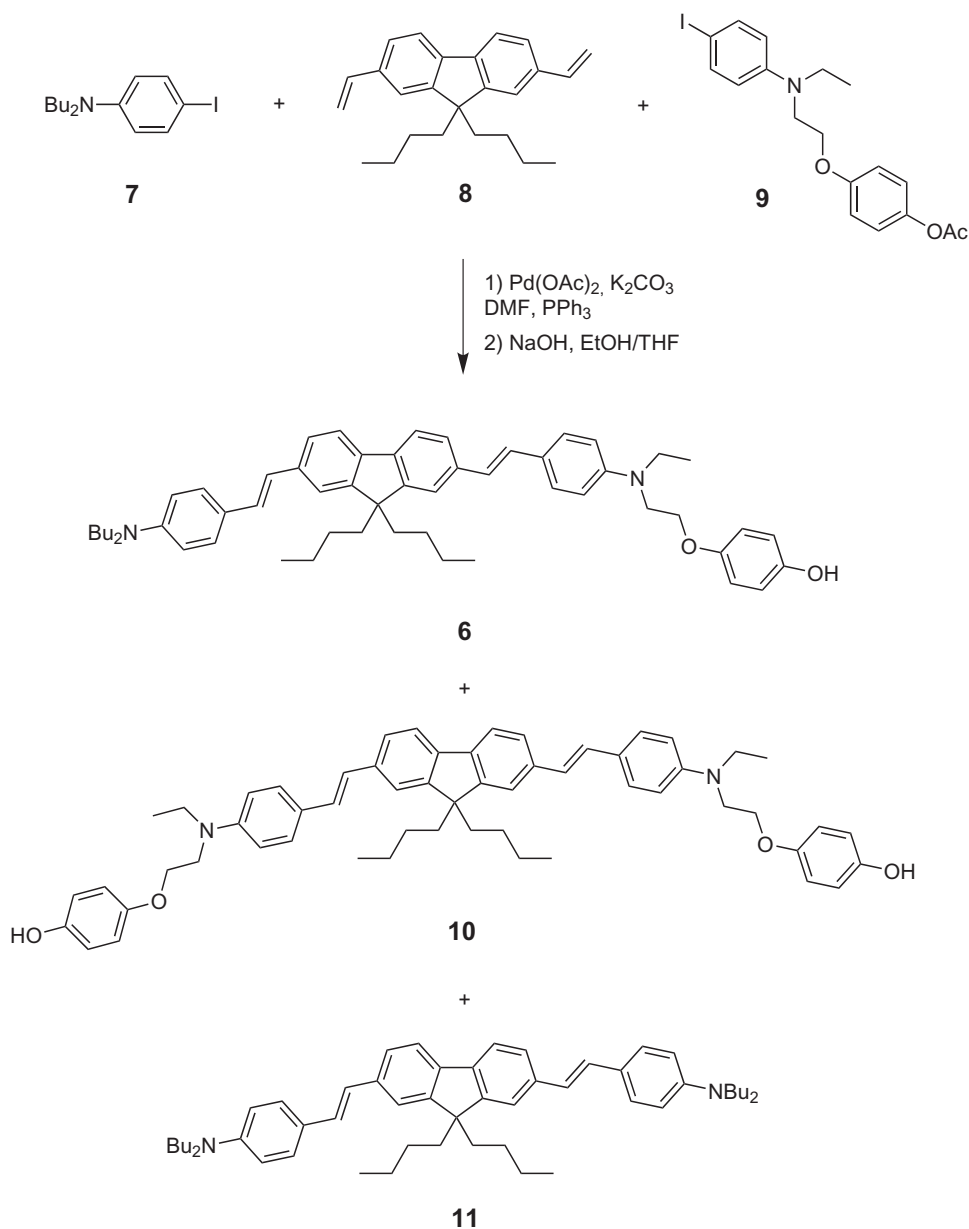
The triad design was meant to take advantage of FRET in order to promote 2P induced production of singlet oxygen by quenching of the porphyrin triplet state subsequent to its sensitization *via* energy transfer from the strong 2P absorbers (Scheme 1). The quadrupolar chromophore is known to show large 2PA response in the



Scheme 1. Porphyrin-quadrupole triad **1** for combined 2P induced fluorescence and porphyrin sensitization



Scheme 2. Synthetic pathway depicting the preparation of triad **1**



Scheme 3. Synthesis of quadrupolar two-photon fluorophore **6** by a combinatorial Heck coupling

NIR range (over 1000 GM at 720 nm) as well as large fluorescence emission quantum yield [30]. As shown in Fig. 1, there is a slight overlap of the emission spectrum of the model chromophore with the Soret band of the model tetratolylporphyrin (TTP) as well as a large overlap with the Q-bands. In addition to the proximity ensured within the triad, this provides favorable conditions for efficient energy transfer from the quadrupolar 2PA absorber as a donor to the porphyrin as an acceptor. We stress that we chose a bis-donor quadrupolar chromophore such as it does not engage in electron transfer with the excited porphyrin or quench the porphyrin triplet state by triplet-triplet energy transfer. Such deactivation processes would compete with fluorescence emission and intersystem crossing as well as hamper singlet oxygen generation [31].

Photophysical properties

The photophysical characteristics (including one-photon absorption, fluorescence, singlet oxygen generation and two-photon absorption) of the triad as well as those of its subunits have been investigated in toluene and are summarized in Table 1.

The absorption spectrum of the triad **1** (Fig. 2) is reminiscent of the absorption spectrum of the reference compound tetratolylporphyrin (TTP) where both characteristic Q-bands and Soret band are clearly seen. Their position remains unaffected by the grafting of quadrupolar fluorophore units indicating that no major electronic interaction arises in the ground-state between the porphyrin and the quadrupolar subunits within the

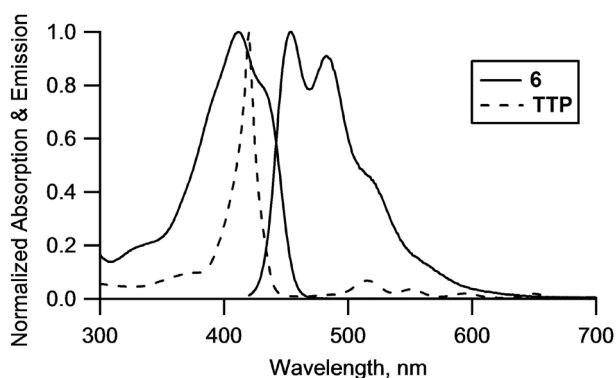


Fig. 1. Absorption and emission spectra of **6** and absorption spectrum of **TTP**

triad. Similarly, no modification of the porphyrin Q-bands is observed compared to the reference compound **TTP**. The low-energy absorption band of the quadrupolar subunit **6** ($\lambda^{\max} = 415$ nm) overlaps with the Soret band (see Fig. 1) of the porphyrin subunit inducing both a broadening and increase in the molar absorption coefficient. We observe an almost perfect additive behavior (see Fig. 2) with a slight narrowing which might possibly be related to a reduced inhomogeneous broadening of the absorption band of the quadrupolar subunits due to the proximity of the bulky **TTP**.

Fluorescence emission spectra were also recorded in toluene. As shown in Fig. 3, excitation of the Q-bands of triad **1** leads to the typical emission of the porphyrin subunit. Moreover, as indicated in Table 1, both the fluorescence quantum yield (0.11) and fluorescence lifetime of the porphyrin (9.3 ns) are retained in triad **1**. Moreover, the singlet oxygen generation quantum yield is found to be unaffected as compared to that of **TTP**. This demonstrates that the photochemistry of the excited states (both singlet and triplet states) of the porphyrin subunit is indeed fully retained in the triad system and that no competing processes (such as electron transfer from the porphyrin excited states) occur which would affect the PDT efficiency. Hence both the fluorescence properties and the sensitizing properties efficiency of the **TTP** subunit are maintained in triad **1** (see Table 1).

Furthermore, as illustrated in Fig. 4, excitation at 422 nm where the Soret band partially overlaps with the

low energy absorption band of the quadrupolar subunits also leads to the characteristic emission of the porphyrin in the red-NIR region at 656 and 722 nm, with only very slight residual emission of the quadrupolar subunit in the blue visible region. This reveals that FRET from the excited quadrupolar subunit is indeed operative. Due to the overlap with the Soret band, it is not possible to excite selectively the quadrupolar subunits of triad **1**. However, by investigating the variation of the fluorescence lifetime of the residual blue-green emission which decreases from 0.90 ns to 0.2 ns, a FRET efficiency of about 80% can be estimated. In addition, we observe that excitation at 422 nm (where the both the quadrupolar and the porphyrin subunits absorb with relative ratio of 14/42) gives rise to the characteristic emission of porphyrin with a fluorescence quantum yield of 0.10 (Table 1). This value is consistent with a FRET efficiency of about 85% from the excited quadrupolar subunits of triad **1** to the porphyrin subunit.

The fluorescence properties of triad **1** and its quadrupolar subunit **6** were also investigated in the solid state. Interestingly both compounds retain fluorescence in the solid state (Fig. 5). Quadrupolar chromophore **6** shows a bright green emission with a red-shifted ($\lambda_{\max} = 530$ nm instead of 455 nm in toluene, see Fig. 5) and broadened emission band as compared to that of the chromophore dissolved in a low polarity solvent such as toluene. This can be interpreted as the effect of polarity and symmetry breaking [32] in the excited state of the quadrupolar chromophore in the solid state. This reveals an environment of medium polarity in the solid state, resulting from the confinement of polarizable quadrupolar chromophores [22]. In contrast, triad **1** shows in the solid state a red-NIR emission characteristic of the porphyrin subunit indicating that FRET is fully operative in the solid state (Fig. 5). A marked broadening of the emission spectra is observed compared to the emission spectrum in solution, most probably due to inhomogeneous broadening.

Two-photon absorption

Thanks to the fluorescence properties of the triad, its two-photon absorption properties were investigated by conducting two-photon excited fluorescence (TPEF) experiments following the well-known methodology

Table 1. Photophysical properties of porphyrin-quadrupole triad **1** and its subunits (**6** and **TTP**) in toluene

Compound	$\lambda_{\text{abs}}^{\max}$, nm	ϵ^{\max} ($10^4 \text{ M}^{-1} \cdot \text{cm}^{-1}$)	$\lambda_{\text{abs}}^{\max}$ (Q-bands), nm	ϵ^{\max} (Q-bands) ($10^4 \text{ M}^{-1} \cdot \text{cm}^{-1}$)	$\lambda_{\text{em}}^{\max}$, nm	λ_{exc} , nm	Φ_f	τ_f^c	Φ_{Δ}^d
TTP	420	42	516, 550, 594, 650	1.7, 0.9, 0.5, 0.5	654, 722		0.11 ^a	9.4	0.66
6	412	7.0	—	—	454		0.77 ^b	0.9	—
1	422	57	517, 552, 594, 650	1.8, 1.0, 0.5, 0.4	656, 722	517, 552, 594, 422	0.11 ^a 0.10 ^a	9.3	0.66

^a Fluorescence quantum yield determined relative to cresyl violet in methanol ($\Phi = 0.54$). ^b Fluorescence quantum yield determined relative to fluorescein in NaOH (0.1 M) ($\Phi = 0.9$). ^c Ex @ 370 nm. ^d Singlet oxygen quantum yield determined in toluene relative to TPP.

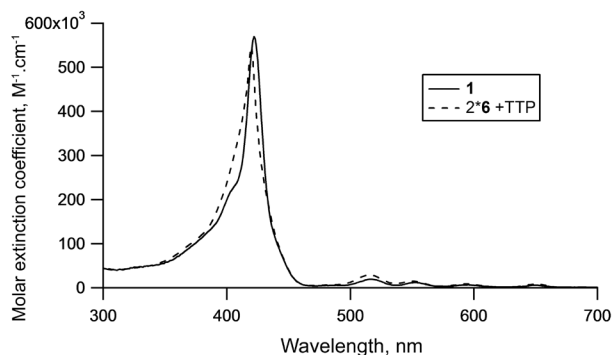


Fig. 2. Absorption spectrum of triad **1** in toluene compared to the additive contribution of quadrupolar and **TTP** porphyrin subunits

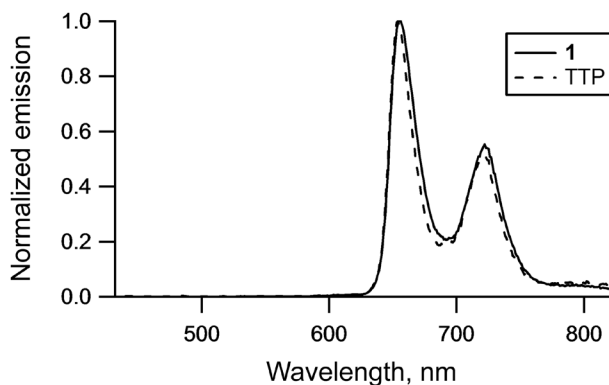


Fig. 3. Emission spectrum of triad of **1** upon excitation of the Q-bands compared to that of **TTP**

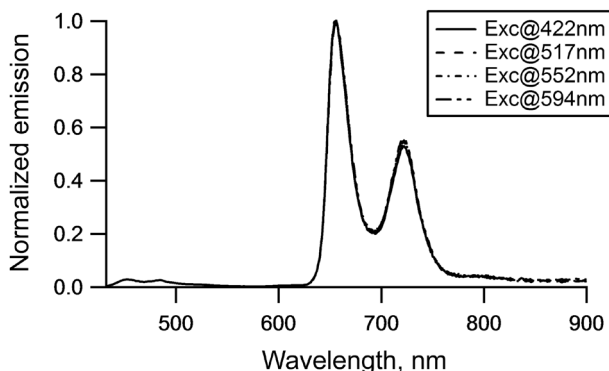


Fig. 4. Emission spectra of triad of **1** upon excitation at different wavelengths

proposed by Webb and collaborators [33]. For comparison purpose, the two-photon absorption properties of the **TTP** and quadrupolar subunit **6** were also investigated. The experimental results are summarized in Table 2. The TPEF experiments were performed in the 680–1000 nm spectral range in the case of blue-green emitting compound **6** and in the range 800–1000 nm for the red-NIR emitting triad **1** and **TTP** to avoid overlap with emission below 800 nm in the latter cases.

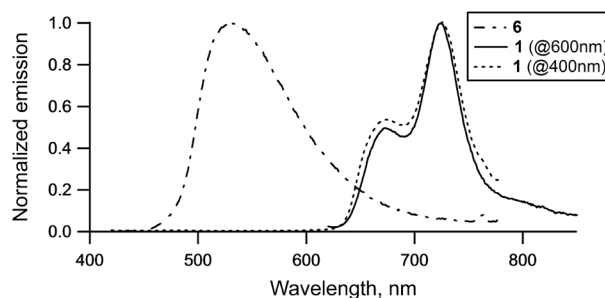


Fig. 5. Emission spectra of quadrupolar subunit **6** ($\lambda_{\text{exc}} = 400$ nm) and triad **1** ($\lambda_{\text{exc}} = 600$ nm and $\lambda_{\text{exc}} = 400$ nm) in the solid state

As shown in Fig. 6, **TTP** is found to show a two-photon absorption cross section of 46 GM at 810 nm. We note that this value is somewhat larger than those reported earlier for the tetraphenylporphyrin [8, 9]. It is indeed closer than that reported for tetrakis(4-sulfonatophenyl) porphyrin diacid at similar wavelength (30 GM) [34]. The TPA spectrum of chromophoric subunit **6** shows the typical behavior of a quadrupolar dye, with a smaller TPA response corresponding to the transition to the lowest strongly one-photon allowed excited state (shoulder at 820 nm) and a much larger TPA response at higher energy (peak at 740 nm) corresponding to the transition to a higher one-photon forbidden but strongly two-photon allowed excited state. As a result, triad **1** is found to show a much larger two-photon absorption response with a local maximum TPA at 810 nm which amounts to 450 GM, corresponding to the additive contribution of two chromophoric subunits **6** and one **TTP**. Hence, triad **1** shows a two-photon absorption response which is one order of magnitude larger than that of **TTP** while fully retaining the fluorescence properties of **TTP** and its sensitizing properties. As such triad **1** is found to combine improved two-photon brightness ($\sigma_2\Phi_i$) and two-photon induced singlet oxygen generation ($\sigma_2\Phi_\Delta$). Of much interest is the realization that whereas the one-photon absorption at 420 nm is mainly dominated by the porphyrin subunit, the two-photon absorption at 810 nm is mainly ensured by the quadrupolar subunits within the triad due to their larger two-photon absorption response at 810 nm (*i.e.* 185 GM per quadrupolar subunit). Moreover, we observe that the TPA spectrum of triad **1** shows good agreement with additive contributions of its quadrupolar and **TTP** subunits (Fig. 6), confirming that the quadrupolar and porphyrin subunits do not interact in the ground state of triad **1** and validating the implemented design.

EXPERIMENTAL

Synthetic procedures

General methods: melting points were measured on Stuart SMP 10. ^1H , ^{13}C and ^{31}P NMR spectra were recorded

Table 2. Two-photon absorption properties of porphyrin-quadrupole triad **1** and its subunits (**6** and **TTP**) in toluene

Compound	$2\lambda_{\text{abs}}^{\text{max}}$, nm	$\lambda_{\text{TPA}}^{\text{max}}$, nm	σ_2^{max} , GM ^a	$\sigma_2^{\text{max}} \rightarrow \Phi_{\text{T}}$, GM ^b	$\sigma_2^{\text{max}} \Phi_{\Delta}$, GM ^c
TTP	840	810	46	5.1	30
6	824	820 (sh) 740	190 1150	146 888	—
1	844	810	450	50	300

^aTwo-photon absorption cross section (1 GM = 10⁻⁵⁰ cm⁴.s.photon⁻¹). ^bTwo-photon brightness. ^cTwo-photon induced singlet oxygen generation cross section.

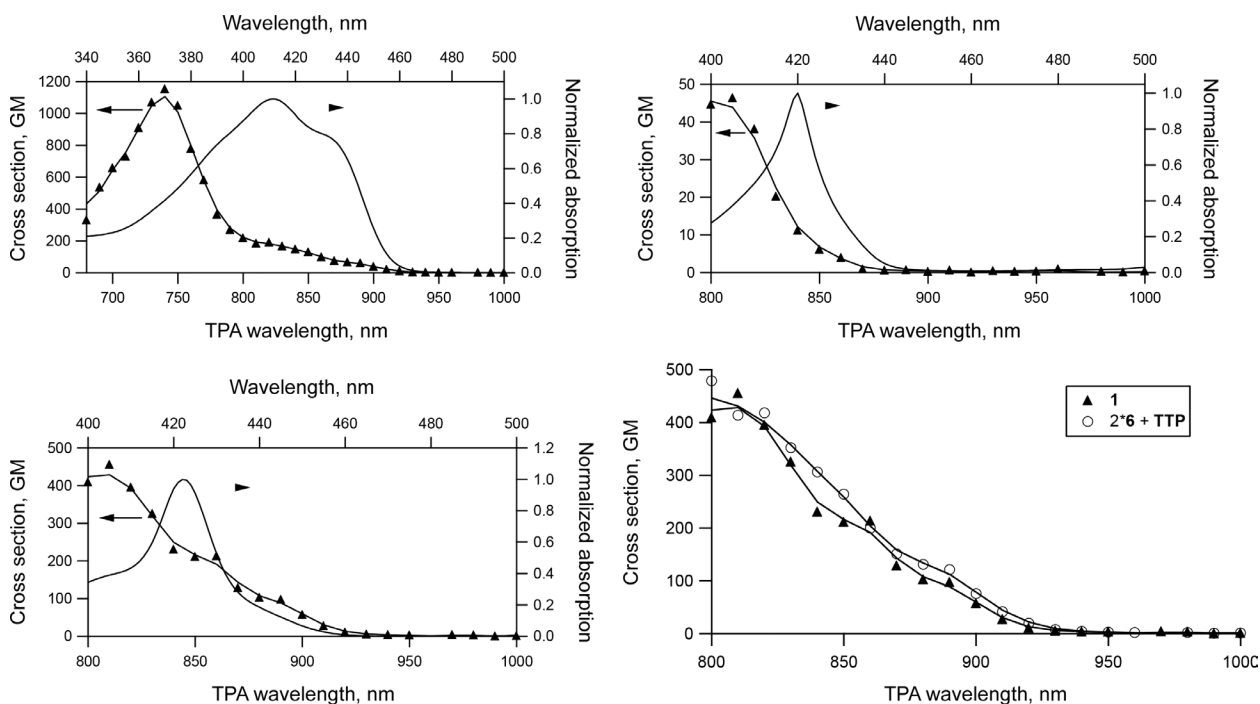


Fig. 6. Two-photon absorption spectra of triad **1** (bottom left), quadrupolar subunit **6** (top left) and **TTP** (top right) in toluene compared with their rescaled one-photon absorption and two-photon absorption spectrum of triad **1** in toluene compared to the additive contribution of quadrupolar and **TTP** porphyrin subunits (bottom right)

on a Bruker Advance I 300 spectrometer at 300 MHz, 75 MHz and 121.4 MHz respectively. Chemical shifts are given in parts per million with respect to solvent residual peak and coupling constant (J) are given in Hz. HRMS spectra were performed by the CESAMO (Bordeaux, France) on a JEOL AccuTOFGCv mass spectrometer using an FD emitter with an emitter voltage of 10 kV. Elemental Analyses were carried out by the CESAMO (Bordeaux, France) or were carried out by the ICSN (CNRS Gif/Yvette, France). Column chromatography was performed on silica gel 60 (40–63 μm , Fluka). Solvents were freshly distilled before use from CaH₂ (toluene, DMF, CH₂Cl₂, and Et₃N) or benzophenone/Na (THF). Compounds **7** and **9** have been prepared according to previously reported procedures [29].

5-(4-Methylcarboxyphenyl)-10,15,20-tris(4-methylphenyl)porphyrin (2). To a mixture of 4-carbomethoxybenzaldehyde (4.1 g, 25 mmole) and 4-tolualdehyde

(7.2 g, 60 mmole) in propionic acid (250 mL) at 120 °C, 5.4 g (80 mmole) of pyrrole was added in one portion. The mixture was refluxed for one hour and left at 4 °C overnight. The precipitate was filtered and rinsed thoroughly with MeOH. The mixture of porphyrins (2.19 g) was chromatographed on silica using CH₂Cl₂ as eluent. (Solubility of the reaction mixture is impeded by large amount of slightly soluble tetratolylporphyrin). After elution of tetratolylporphyrin, the fraction containing the expected product was evaporated and precipitated with a large excess of MeOH. 880 mg of **2** was obtained as a purple powder (yield 6.2%). ¹H NMR (300 MHz, CDCl₃): δ , ppm 8.93 (m, 6H), 8.83 (d, J = 4.9 Hz, 2H), 8.49 (d, J = 8.3 Hz, 2H), 8.36 (d, J = 8.3 Hz, 2H), 8.15 (d, J = 7.8 Hz, 6H), 7.60 (d, J = 7.8 Hz, 6H), 4.16 (s, 3H), 2.76 (s, 9H), -2.70 (s, 2H).

5-(4-Hydroxymethylphenyl)-10,15,20-tris(4-methylphenyl)porphyrin (3). To a stirred solution of

2 (500 mg, 0.7 mmole) in freshly distilled THF at 0°C, 250 mg of LiAlH₄ was added in small portions. The reaction mixture was stirred for 3 h at room temperature and then hydrolyzed by slow addition of 6 mL of MeOH at 0°C. Then, 15 mL of a saturated aqueous solution of Rochelle's salt (sodium and potassium tartrate) was added and the product was extracted with CHCl₃ (250 mL). The organic phase was washed successively with the tartrate solution and water. Drying over Na₂SO₄ and evaporation afforded **3** as a violet powder (403 mg, 84%). ¹H NMR (300 MHz, CDCl₃): δ, ppm 8.90 (d, *J* = 4.7 Hz, 4H), 8.89 (bs, 4H), 8.86 (d, *J* = 5.1 Hz, 4H), 8.25 (d, *J* = 8 Hz, 2H), 8.14 (d, *J* = 7.7 Hz, 6H), 7.79 (d, *J* = 8 Hz, 2H), 7.59 (d, *J* = 7.7 Hz, 6H), 5.11 (d, *J* = 5 Hz, 2H), 2.75 (s, 9H), 2.00 (t, *J* = 5 Hz, 1H), -2.73 (s, 2H).

5-(4-Formylphenyl)-10,15,20-tris(4-methylphenyl) porphyrin (4). A suspension containing 340 mg of alcohol **3** (0.5 mmoles) and 500 mg of MnO₂ in 30 mL of CH₂Cl₂ was refluxed for 4 h. The reaction could be monitored by TLC on silica (eluent CHCl₃). The crude reaction mixture was filtered through a small silica pad, eluting with CH₂Cl₂, evaporated to dryness and afforded 209 mg of aldehyde **4** (61% yield). ¹H NMR (300 MHz, CDCl₃): δ, ppm 10.42 (s, 1H), 8.94 (d, *J* = 4.7 Hz, 4H), 8.93 (bs, 4H), 8.80 (d, *J* = 4.7 Hz, 4H), 8.44 (d, *J* = 7.9 Hz, 2H), 8.31 (d, *J* = 7.9 Hz, 2H), 8.14 (d, *J* = 8.1 Hz, 6H), 7.60 (d, *J* = 8.1 Hz, 6H), 2.75 (s, 9H), -2.71 (s, 2H).

Compound 5. 5 mL of a 0.18 M solution of phosphorodichloridothioic hydrazide, 1-methyl-(MMH-PSCl₂) in CHCl₃ was added to a solution of **4** (324 mg, 0.47 mmole) in dry dichloromethane (50 mL), and let 24 h at room temperature. Concentration to a final volume of 15 mL and precipitation with petroleum ether afforded a green precipitate which was collected by filtration. A rapid filtration on a 10 cm silica pad was carried out, eluting with CH₂Cl₂ and a trace amount of Et₃N and thus afforded 310 mg of a violet powder after evaporation (yield 78%). The product was used without further purification for the next reaction step. ¹H NMR (300 MHz, CDCl₃): δ, ppm 8.93–8.88 (AB system, *J* = 4.7 Hz, 4H), 8.91 (bs, 4H), 8.32 (d, *J* = 8.3 Hz, 2H), 8.16 (d, *J* = 8.3 Hz, 2H), 8.14 (d, *J* = 8 Hz, 6H), 8.07 (d, *J* = 2.4 Hz, 1H), 7.60 (d, *J* = 8 Hz, 6H), 3.70 (d, *J* = 13.9 Hz, 3H), 2.75 (s, 9H), -2.70 (s, 2H). ³¹P NMR (121.4 MHz, CDCl₃): δ, ppm 63.38.

Triad 1. Cs₂CO₃ (300 mg, 0.92 mmole) was added to a mixture of compound **5** (100 mg, 0.12 mmole) and compound **6** (200 mg, 0.25 mmole) in 10 mL of dry THF. The reaction mixture was heated for 5 h at 60°C and the solvent was evaporated. Column chromatography on neutral alumina (grade IV) with CH₂Cl₂ afforded compound **1** as a brown powder, 235 mg. Yield 83%. Anal. calcd. for C₁₅₉H₁₇₃N₁₀O₄PS.H₂O; C: 81.22, H: 7.42, N: 5.96, S: 1.36%. Found C: 81.43, H: 7.19, N: 5.71, S: 1.39. MS (MALDI-TOF): *m/z* 2351.3 (calcd. for [M + H]⁺ 2351.3). ¹H NMR (300 MHz, CDCl₃): δ, ppm 8.94 (m, 8H), 8.31 (d, *J* = 8.1 Hz, 2H), 8.15 (m, 8H), 8.03 (bs,

1H, CH=N), 7.61 (m, 10H), 7.46 (m, 14H), 7.32 (d, *J* = 9 Hz, 4H), 7.12 (d, *J* = 16.2 Hz, 2H), 7.10 (d, *J* = 16.2 Hz, 2H), 7.01 (d, *J* = 16.2 Hz, 4H), 6.93 (d, *J* = 9 Hz, 4H), 6.73 (d, *J* = 8.8 Hz), 6.68 (d, *J* = 8.8 Hz), 4.15 (t, *J* = 6.2 Hz), 3.77 (t, *J* = 6.2 Hz, 4H), 3.54 (d, *J*_{H-P} = 10.2 Hz, 3H), 3.51 (m, 4H), 3.45 (m, 8H), 2.75 (bs, 9H), 2.02 (m, 8H), 1.64 (m, 16H), 1.42 (m, 8H), 1.24 (t, *J* = 7.7 Hz, 6H), 1.13 (m, 8H), 1.02 (t, *J* = 7.3 Hz, 12 H), 0.71 (t, *J* = 7.3 Hz, 12H). ³¹P NMR (121.42 MHz, CDCl₃): δ, ppm 64.29.

Compound 6. The Heck dissymmetrical coupling was performed by mixing 2,7-diethenyl-9,9-dibutyl-9H-fluorene (1.36 g, 4.11 mmole), 4-[2-[ethyl(4-iodophenyl)amino]ethoxy]phenyl acetate (2 g, 4.70 mmole), 4-iodo-*N,N*-dibutylaniline (1.55 g, 4.70 mmole), K₂CO₃ (1.45 g), tetrabutylammonium bromide (2.78 g), triphenylphosphine (237 mg) and Pd(OAc)₂ (110 mg) in DMF (35 mL) under an Ar atmosphere. The mixture was heated at 50°C under Ar for 24 h. The DMF was removed by evaporation under reduced pressure and the residue was chromatographed on silica using an increasing gradient of petroleum ether/CH₂Cl₂ (from 70/30 to 0/100) affording 1.25 g of a yellow-green powder which was used directly for the deprotection step. The compound was dissolved in a mixture of THF (50 mL) and EtOH (25 mL) and 10 mL of 0.5 M NaOH was added. The solution was stirred 20 min at room temperature and 0.5 M HCl aqueous solution (12 mL) was added. The solution was taken up in diethyl ether and washed with 10% NaHCO₃ solution, dried and evaporated. The residue was chromatographed on silica using a petroleum ether/CH₂Cl₂ (40/60) mixture and afforded **6** as a yellow powder (620 mg, 19% yield from the 2,7-diethenyl-9,9-dibutyl-9H-fluorene precursor). By NMR the presence of a small amount (*ca.* 10%) of minor isomers could be detected. mp 65–67°C. ¹H NMR (300 MHz, CDCl₃): δ, ppm 7.65 (d, *J* = 8.1 Hz, 2H), 7.46 (m, 8H), 7.13 (d, *J* = 16.2 Hz, 2H), 7.03 (d, *J* = 16.2 Hz, 1H), 7.01 (d, *J* = 16.2 Hz, 1H), 6.81 (m, 6H), 6.78 (d, *J* = 8.1 Hz, 2H), 6.68 (d, *J* = 8.1 Hz, 2H), 4.50 (s, 1H), 4.13 (t, *J* = 6.1 Hz, 2H), 3.77 (t, *J* = 6.1 Hz, 2H), 3.55 (q, *J* = 7.0 Hz, 2H), 3.34 (t, *J* = 6.9 Hz, 4H), 2.05 (m, 4H), 1.64 (m, 4H), 1.41 (m, 4H), 1.27 (t, *J* = 7.0 Hz, 3H), 1.14 (m, 4H), 1.01 (t, *J* = 7.2 Hz, 6H), 0.73 (t, *J* = 7.3 Hz, 6H), 0.71 (m, 4H). ¹³C NMR (100 MHz, CDCl₃): δ, ppm 153.16, 151.68, 149.88, 140.28, 140.06, 137.32, 137.06, 128.92, 128.32, 128.02, 127.92, 126.66, 125.94, 125.23, 125.01, 124.63, 120.44, 120.34, 119.82, 116.31, 115.83, 112.11, 111.94, 66.36, 55.03, 51.05, 50.02, 45.94, 40.69, 29.77, 26.21, 23.39, 20.62, 14.28, 14.08, 12.64. Anal. calcd. for C₅₅H₆₈N₂O₂; C: 83.71, H: 8.69, N: 3.55%. Found C: 83.45, H: 8.39, N: 3.41. HRMS (FD): *m/z* calcd. for C₅₅H₆₈N₂O₂ 788.5281. Found 788.5255.

Compound 8. A commercial vinylmagnesium bromide solution (25 mL, 1 M in THF) was slowly added under argon to a degazed mixture of 2,7-diiodo-9,9-dibutyl-9H-fluorene (4 g, 7.54 mmole) and PdCl₂dppf (246 mg, 302 mmole) in dry THF (50 mL) at room

temperature. The suspension was stirred for 12 h and hydrolyzed with ammonium chloride solution (10% in water). Extraction with diethyl ether and subsequent column chromatography on silica (eluent: petroleum ether) afforded a white solid (1.92 g, 77%) that had to be used rapidly in the following step due to its polymerization ability. mp 75 °C. $^1\text{H NMR}$ (300 MHz, CDCl_3): δ , ppm 7.62 (d, $J = 7.8$ Hz, 2H), 7.39 (d, $J = 7.8$ Hz, 2H), 7.36 (s, 2H), 6.80 (dd, $J = 11.8$ Hz, $J = 17.7$ Hz, 2H), 5.79 (d, $J = 17.4$ Hz, 2H), 5.26 (d, $J = 11.4$ Hz, 2H), 1.97 (m, 4H), 1.08 (m, 4H), 0.67 (t, $J = 7.2$ Hz, 6H), 0.62 (m, 4H).

Photophysical studies

All photophysical properties were analyzed with freshly prepared air equilibrated solutions at room temperature (293 K). UV-vis absorption spectra were recorded using a Jasco V-570 spectrophotometer. Steady-state fluorescence measurements were performed on dilute solutions (optical density <0.1) contained in standard 1 cm quartz cuvettes using a Horiba (FluoroLog or FluoroMax) spectrofluorimeter in photon-counting mode. Fully corrected emission spectra were obtained for each compound at $\lambda_{\text{ex}} = \lambda_{\text{abs}}^{\text{max}}$ with an optical density at $\lambda_{\text{ex}} \leq 0.1$ to minimize internal absorption. Fluorescence quantum yields were measured according to literature procedures [35], using fluorescein in 0.1 M NaOH ($\Phi_{\text{f}} = 0.9$), or cresyl violet in MeOH ($\Phi_{\text{f}} = 0.54$). Measurement of singlet oxygen quantum yields (Φ_{Δ}) was performed on a Fluorolog-3 (Horiba Jobin Yvon) spectrometer using a 450W Xe lamp. The emission at 1272 nm was detected using a liquid nitrogen cooled Ge-detector model (EO-817L, North Coast Scientific Co). Singlet oxygen quantum yields Φ_{Δ} were determined in toluene solutions, using tetraphenylporphyrin (TPP) in toluene as reference solution ($\Phi_{\Delta \text{ TPP}} = 0.68$) and were estimated from $^1\text{O}_2$ luminescence at 1272 nm [36]. Fluorescence decays were measured in a time-correlated single photon counting (TCSPC) configuration, under excitation from selected nanoLED (370, 455 or 570 nm). The instrument response was determined by measuring the light scattered by a Ludox suspension. The lifetime values were obtained from the reconvolution fit analysis of the decay profiles; the quality of the fits was judged by the reduced χ^2 value ($\chi^2 < 1.1$). The reported lifetimes are within ± 0.1 ns.

Two-photon absorption

TPA cross sections (σ_2) were determined from the two-photon excited fluorescence (TPEF) cross sections ($\sigma_2\Phi_{\text{f}}$) and the fluorescence emission quantum yield (Φ_{f}). TPEF cross sections were measured relative to fluorescein in 0.01 M aqueous NaOH for 715–980 nm, using the well-established method described by Xu and Webb and the appropriate solvent-related refractive index corrections [37]. The quadratic dependence of the fluorescence intensity on the excitation power was checked for each sample and all wavelengths, indicating

that the measurements were carried out in intensity regimes where one-photon absorption, saturation or photodegradation did not occur.

Measurements were conducted using excitation sources delivering fs pulses. This is preferred in order to avoid excited state absorption during the pulse duration, a phenomenon which has been shown to lead to overestimated TPA cross section values. To span the 700–980 nm range, a Nd:YLF-pumped Ti:sapphire oscillator was used generating 150 fs pulses at a 76 MHz rate. The excitation was focused into the cuvette through a microscope objective (10X, NA 0.25). The fluorescence was detected in epifluorescence mode *via* a dichroic mirror (Chroma 675dcxru) and a barrier filter (Chroma e650sp-2p) by a compact CCD spectrometer module BWTek BTC112E. Total fluorescence intensities were obtained by integrating the corrected emission. The experimental uncertainty of the action cross section values determined by this method has been estimated to be $\pm 10\%$.

CONCLUSION

In this work, we demonstrate that the engineering strategy which relies on covalently grafting quadrupolar chromophoric subunits based on a fluorenyl core and having electron-donating end-groups onto a TTP porphyrin is effective in both ensuring improved two-photon absorption in the NIR region of interest for bioapplications (thanks to antenna effect) as well as maintaining the excellent sensitizing properties of the porphyrin subunit and its fluorescence properties. As a result, the triad model compound shows both enhanced two-photon brightness and two-photon induced singlet oxygen generation (both being increased by an order of magnitude as compared to the single porphyrin). This strategy will be extended to other triad systems with quadrupolar chromophoric subunits showing larger two-photon absorption cross sections. This could be done in particular by keeping the main design (*i.e.* fluorene core and donating end-groups) but extending and tuning the π -connector [30].

Further developments will include encapsulation of the triad into biocompatible nanocarriers to preserve their photophysical properties while ensuring bioavailability and offering the possibility to include surface of targeting units for cancer therapy. Such cooperative triad system would offer major prospect for theranostics.

Acknowledgements

We thank the Conseil Régional d'Aquitaine for financial support (Chaire d'Accueil grant to MBD). This study was achieved within the context of the Laboratory of Excellence TRAIL ANR-10-LABX-57. The authors are grateful to Jean-Pierre Majoral for generous gift of MMH-PSC12.

REFERENCES

- Dougherty TJ, Gomer CJ, Henderson BW, Jori G, Kessel D, Koberlik M, Moan J and Peng Q. *J. Nat. Canc. Inst.* 1998; **90**: 889–905.
- McDonald IJ and Dougherty TJ. *J. Porphyrins Phthalocyanines* 2001; **5**: 105–129.
- Dougherty TJ. *J. Clin. Laser Med. Surg.* 2002; **20**: 3–7.
- (a) Bhawalkar JD, Kumar ND, Zhao CF and Prasad PN. *J. Clin. Laser Med. Surg.* 1997; **15**: 201–204. (b) Starkey JR, Rebane AK, Drobizhev MA, Meng F, Gong A, Elliott A, McInnerney K and Spangler CW. *Clin. Cancer Res.* 2008; **14**: 6564–6573. (c) Gary-Bobo M, Mir Y, Rouxel C, Brevet D, Basile I, Maynadier M, Vaillant O, Mongin O, Blanchard-Desce M, Morère A, Garcia M, Durand JO and Raehm L. *Angew. Chem., Int. Ed.* 2011; **50**: 11425–11429.
- Collins HA, Khurana M, Moriyama EH, Mariampillai A, Dahlstedt E, Balaz M, Kuimova MK, Drobizhev M, Yang VXD, Phillips D, Rebane A, Wilson BC and Anderson HL. *Nat. Photonics* 2008; **2**: 420–424.
- Xu C, Zipfel W, Shear JB, Williams RM and Webb WW. *Proc. Natl. Acad. Sci. USA* 1996; **93**: 10763–10768.
- Robin AC, Gmouh S, Mongin O, Jouikov V, Werts MHV, Gautier C, Slama-Schwok A and Blanchard-Desce M. *Chem. Comm.* 2007; 1334–1336.
- Drobizhev M, Karotki A, Kruk M and Rebane A. *Chem. Phys. Lett.* 2002; **355**: 175–182.
- Makarov NS, Drobizhev M and Rebane A. *Opt. Exp.* 2008; **16**: 4029–4047.
- (a) Ogawa K, Ohashi A, Kobuke Y, Kamada K and Ohta K. *J. Am. Chem. Soc.* 2003; **125**: 13356–13357. (b) Drobizhev M, Stepanenko Y, Dzenis Y, Karotki A, Rebane A, Taylor PN and Anderson HL. *J. Am. Chem. Soc.* 2004; **126**: 15352–15353. (c) Achelle S, Couleaud P, Baldeck P, Teulade-Fichou MP and Maillard P. *Eur. J. Org. Chem.* 2011; **2011**: 1271–1279. (d) Hammerer F, Achelle S, Baldeck P, Maillard P and Teulade-Fichou MP. *J. Phys. Chem. A* 2011; **115**: 6503–6508. (e) Balaz M, Collins HA, Dahlstedt E and Anderson HL. *Org. Biomol. Chem.* 2009; **7**: 874–888.
- (a) Kim DY, Ahn TK, Kwon JH, Kim D, Ikeue T, Aratani N, Osuka A, Shigeiwa M and Maeda S. *J. Phys. Chem. A* 2005; **109**: 2996–2999. (b) Ahn TK, Kim KS, Kim DY, Noh SB, Aratani N, Ikeda C, Osuka A and Kim D. *J. Am. Chem. Soc.* 2006; **128**: 1700–1704. (c) Pawlicki M, Morisue M, Davis NKS, McLean DG, Haley JE, Beuerman E, Drobizhev M, Rebane A, Thompson AL, Pascu SI, Accorsi G, Armaroli N and Anderson HL. *Chem. Sci.* 2012; **3**: 1541–1547.
- Drobizhev M, Karotki A, Kruk M, Mamardashvili NZ and Rebane A. *Chem. Phys. Lett.* 2002; **361**: 504–512.
- (a) Rath H, Sankar J, Prabhu Raja V, Chandrashekar TK, Nag A and Goswami D. *J. Am. Chem. Soc.* 2005; **127**: 11608–11609. (b) Misra R, Kumar R, Chandrashekar TK, Nag A and Goswami D. *Org. Lett.* 2006; **8**: 629–631.
- Kim KS, Lim JM, Osuka A and Kim D. *J. Photochem. Photobiol. C: Photochem. Rev.* 2008; **9**: 13–28.
- Collini E, Mazzucato S, Zerbetto M, Ferrante C, Bozio R, Pizzotti M, Tessoro F and Ugo R. *Chem. Phys. Lett.* 2008; **454**: 70–74.
- Esipova TV and Vinogradov SA. *J. Org. Chem.* 2014; **79**: 8812–8825.
- Mongin O, Sankar M, Charlot M, Mir Y and Blanchard-Desce M. *Tet. Lett.* 2013; **54**: 6474–6478.
- (a) Brousmiche DW, Serin JM, Fréchet JM, He GS, Lin TC, Chung SJ and Prasad PN. *J. Am. Chem. Soc.* 2003; **125**: 1448–1449. (b) Brousmiche DW, Serin JM, Fréchet JM, He GS, Lin TC, Chung SJ, Prasad PN, Kannan R and Tan LS. *J. Phys. Chem. B* 2004; **108**: 8592–8600.
- (a) Brinas RP, Troxler T, Hochstrasser RM and Vinogradov SA. *J. Am. Chem. Soc.* 2005; **127**: 11851–11862. (b) Finikova OS, Troxler T, Senes A, DeGrado WF, Hochstrasser RM and Vinogradov SA. *J. Phys. Chem. A* 2007; **111**: 6977–6990.
- (a) Finikova OS, Lebedev AY, Aprelev A, Troxler T, Gao F, Garnacho C, Muro S, Hochstrasser RM and Vinogradov SA. *Chem. Phys. Chem.* 2008; **9**: 1673. (b) Lebedev AY, Troxler T and Vinogradov SA. *J. Porphyr. Phthalocyanines* 2008; **12**: 1261.
- Mongin O, Tathavarty RK, Werts MHV, Caminade AM, Majoral JP and Blanchard-Desce M. *Chem. Commun.* 2006; 915–917.
- Mongin O, Pla-Quintana A, Terenziani F, Drouin D, Le Droumaguet C, Caminade AM, Majoral JP and Blanchard-Desce M. *New. J. Chem.* 2007; **31**: 1354–1367.
- Guo M, Varnavski O, Narayan A, Mongin O, Majoral JP, Blanchard-Desce M and Goodson T. *J. Phys. Chem. A*, 2009; **113**: 4763–4771.
- (a) Terenziani F, Parthasarathy V, Pla-Quintana A, Maishal T, Caminade AM, Majoral JP and Blanchard-Desce M. *Angew. Chem. Int. Ed.* 2009; **48**: 8691–8694. (b) Robin AC, Parthasarathy V, Pla-Quintana A, Mongin O, Terenziani F, Caminade AM, Majoral JP and Blanchard-Desce M. *Proceedings of SPIE* 2010; 7774 (Linear and Nonlinear Optics of Organic Materials X), 77740N/1–77740N/8.
- (a) Cueto Diaz E, Picard S, Chevasson V, Daniel J, Hugues V, Mongin O, Genin E and Blanchard-Desce M. *Org. Lett.* 2015; **17**: 102–105. (b) Cueto Diaz EJ, Picard S, Klausen M, Hugues V, Pagano

- P, Genin E and Blanchard-Desce M. *Chem. Eur. J.* 2016; **22**: 10848–10859.
26. Picard S, Cueto-Diaz E, Genin E, Clermont G, Acher F, Ogden D and Blanchard-Desce M. *Chem. Commun.* 2013; **49**: 10805–10807.
27. (a) Adler AD, Longo FR, Finarelli JD, Goldmacher J, Assour J and Korsakoff L. *J. Org.Chem.* 1967; **32**: 476. (b) Tomé J, Neves M, Tomé A, Cavaleiro J, Mendonça A, Pegado I, Duarte R and Valdeira M. *Bioorg. Med. Chem.* 2005; **13**: 3878–3888.
28. (a) Zhang X, Hou L, Cnossen A, Coleman AC, Ivashenko O, Rudolf P, Van Wees BJ, Browne WR and Feringa BL. *Chem. Eur. J.* 2011; **17**: 8957–8964. (b) Wennerström O, Ericsson H, Raston I, Svensson S and Pimlott W. *Tetrahedron Lett.* 1989; **30**: 1129–1132.
29. Rouxel C, Charlot M, Mongin O, Krishna TR, Caminade AM, Majoral JP and Blanchard-Desce M. *Chem. Eur. J.* 2012; **18**: 16450–16462.
30. Mongin O, Porrès L, Charlot M, Katan C and Blanchard-Desce M. *Chem. Eur. J.* 2007; **13**: 1481–1498.
31. Finikova OS, Chen P, Ou Z, Kadish KM and Vinogradov SA. *J. Photochem. Photobiol., A* 2008; **198**: 75–84.
32. Terenziani F, Painelli A, Katan C, Charlot M and Blanchard-Desce M. *J. Am. Chem. Soc.* 2006; **128**: 15742–15755.
33. (a) Xu C and Webb WW. *J. Opt. Soc. Am. B* 1996; **13**: 481–491. (b) Albota MA, Xu C and Webb WW. *Appl. Opt.* 1998; **37**: 7352–7356.
34. Collini E, Ferrante C and Bozio R. *J. Phys. Chem. B* 2005; **109**: 2–5.
35. (a) Eaton DF. *Pure & Appl. Chem.* 1988; **60**: 1107–1114. (b) Crosby GA and Demas JN. *J. Phys. Chem.* 1971; **75**: 991–1024.
36. Ganzha VA, Gurinovich GP, Dzhagarov BM, Egorova GD, Sagun EI and Shul'ga MJ. *J. Appl. Spectrosc.* 1989; **50**: 402–406.
37. Werts MHV, Nerambourg N, Pelegry D, Grand YL and Blanchard-Desce M. *Photochem. Photobiol. Sci.* 2005; **4**: 531–538.